CHIN. PHYS. LETT. Vol. 38, No. 1 (2021) 016601

Bidirectional and Unidirectional Negative Differential Thermal Resistance Effect in a Modified Lorentz Gas Model

Yu Yang(杨宇), XiuLing Li(李秀玲)*, and Lifa Zhang(张力发)

NNU-SULI Thermal Energy Research Center (NSTER) and Center for Quantum Transport and Thermal Energy Science (CQTES), School of Physics and Technology, Nanjing Normal University, Nanjing 210023, China

(Received 6 October 2020; accepted 18 November 2020; published online 6 January 2021)

Recently, the negative differential thermal resistance effect was discovered in a homojunction made of a negative thermal expansion material, which is very promising for realizing macroscopic thermal transistors. Similar to the Monte Carlo phonon simulation to deal with grain boundaries, we introduce positive temperature-dependent interface thermal resistance in the modified Lorentz gas model and find negative differential thermal resistance effect. In the homojunction, we reproduce a pair of equivalent negative differential thermal resistance effects in different temperature gradient directions. In the heterojunction, we realize the unidirectional negative differential thermal resistance effect, and it is accompanied by the super thermal rectification effect. Using this new way to achieve high-performance thermal devices is a new direction, and will provide extensive reference and guidance for designing thermal devices.

DOI: 10.1088/0256-307X/38/1/016601

Operations of electronic and optical devices are often accompanied by waste heat, which will greatly affect performance of the devices, or even destroy them. Therefore, research on thermal transport process in devices is of great significance, and a series of important thermal phenomena have been gradually discovered, such as thermal rectification effect,[1−7] thermal Hall effect,[8−10] negative differential thermal resistance (NDTR) effect.[11−17] Recently, the thermal diode designed based on the thermal rectification effect has been proved in experiment,[18,19] but the thermal transistor has not been confirmed. Similar to the electronic transistor, the NDTR effect is considered to be an important means to realize thermal transistors, and has been theoretically predicted to exist in the homojunction or heterojunction system.[11,12,17]

He *et al.* discussed the NDTR effect in the one-dimensional heterogeneous atomic chain model and earlier pointed out that the NDTR effect comes from a positive temperature-dependent interface thermal resistance (ITR).[12] However, in previous theories and experiments, most of the ITR shows a negative temperature dependence, which means that the ITR decreases with increasing interface temperature and interface pressure.[20−31] This is the reason why thermal transistors based on the NDTR effect have not been realized experimentally. This year, we discovered a macroscopic positive temperature-dependent ITR, and the accompanied macroscopic negative differential thermal resistance effect was observed.[17] We use negative thermal expansion material to construct a homogenous junction: the volume of the material expands at low temperature to make the interface squeeze; the volume of the material shrinks at high temperature to make the interface separate. It is very gratifying that the macroscopic positive temperature-dependent ITR is easy to manufacture in experiment. This discovery expands the types of experimentally adjustable ITR, which is of great significance for us to realize the thermal transistor.

The Lorentz gas model is usually used to simulate the thermal transport process, and many interesting results have been discovered and clearly explained.[32−37] Here, the modified Lorentz gas model will be used to study the homogenous/heterojunction thermal transport process with the interface shown in Fig. 1(a). Schematic diagrams of the modified Lorentz gas model are shown in Figs. 1(b) and 1(c). We made two changes to the traditional Lorenz gas model: (i) A static disk scatterer is introduced into the modified Lorentz gas model. Similar to the previous studies,[33−36] this change ensures thermal stability and adjusts the thermal conductivity of the model. (ii) Introducing the interface reflection probability P into the modified Lorentz gas model, particle will transmit or reflect when they cross the interface. The interface is represented by the green area in the schematic diagram, but its length is ignored in simulation, and only an interface reflection probability caused by the positive temperature-dependent interface thermal re-

Supported by the National Natural Science Foundation of China (Grant Nos. 11975125 and 21803031), the Postgraduate Research & Practice Innovation Program of Jiangsu Province (Grant No. KYCX20 1229), and the Natural Science Foundation of the Jiangsu Higher Education Institution of China (Grant No. 18KJB150022).

*Corresponding author. Email: xlli@njnu.edu.cn

© 2021 Chinese Physical Society and IOP Publishing Ltd

sistance is introduced into the model. This setting is very similar to using Monte Carlo simulation to process the BTE equation with grain boundary or internal boundary structure.[34,38,39]

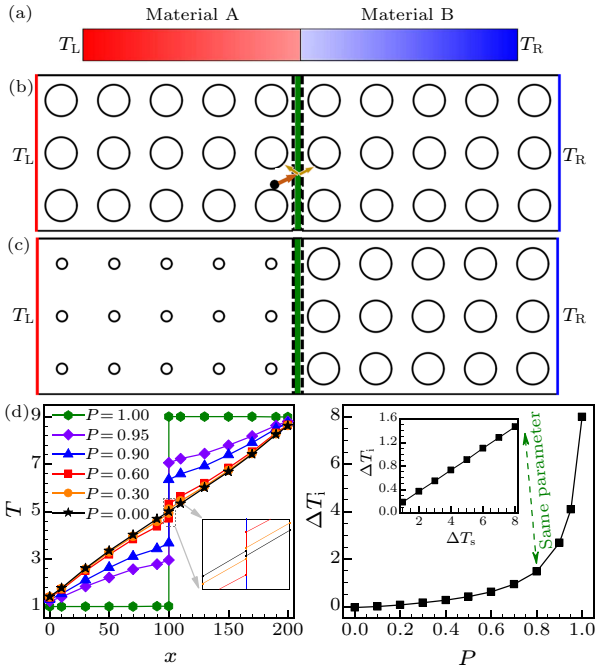

Fig. 1. (a) Schematic diagram of the macroscopic homojunction/heterojunction thermal transport model. (b) and (c) Schematic diagram of the modified Lorentz gas model for homojunction and heterojunction. The model space is a rectangle of total length L and width D, and static circular scattering media having a radius R are arranged internally (totally N: n_x rows, n_y columns). The setting of the model in (a) and (b) is as follows: $L = 200$, $D = 60$, $n_x = 3$, $n_y = 10$, $R_R = 6$, $R_L = 6(2)$. The green area between the dashed lines indicates the interface area. (c) Temperature distribution along the transmission direction with different interface reflection probabilities, where $T_L = 1$, $T_R = 9$. The temperature is approximately linearly distributed in the material. (d) The interface temperature jump as a function of the interface reflection probability. In the inset, we give the relationship between the external temperature difference and the interface temperature jump in a constant interface reflection probability ($P = 0.8$).

The moving particle in the model is emitted from a random location of the thermal source, and the speed distribution satisfies the following conditions:[33–37]

$$P(v_\parallel) = \frac{|v_\parallel|}{T} e^{-v_\parallel^2/(2T)}, \tag{1}$$

$$P(v_\perp) = \frac{1}{\sqrt{2\pi T}} e^{-v_\perp^2/(2T)}, \tag{2}$$

where $v_\parallel$, $v_\perp$ and T are the x-, y-axis component of the velocity and the temperature of thermal source. Specially, we use a dimensionless unit, the Boltzmann constant k_B and the particle mass m are set to 1. At a certain moment, the thermal source initially emits a particle into the system, after which the particle moves continuously, and elastically collides with the boundary (not including the interface) and the scattering medium until it moves to the side of thermal source to be absorbed. The thermal source then releases another particle and repeats the previous process. In order to calculate the temperature distribution in the model, we divide the space into a number of thin strips, and the average kinetic energy of each region is obtained by statistics. Then the temperature distribution T_m in the transmission direction, the steady thermal flow J, and the thermal conductivity κ_{eff} can be calculated by[36,37]

$$T_m = \frac{2}{3} E_m, \tag{3}$$

$$J = \frac{\Delta E}{t}, \tag{4}$$

$$\kappa_{\text{eff}} = \frac{LJ}{D\Delta T}. \tag{5}$$

Here T_m and E_m represent the temperature and average kinetic energy of the mth region, ΔE and ΔT represent the energy change and the temperature difference of the thermal sources, L and D represent the total length and width of the system. The effective thermal conductivity (κ_{eff}) mentioned above refers to the average thermal conductivity of the entire homojunction/heterojunction. The temperature profile is shown in Fig. 1(d). The jump of temperature at the interface is very obvious, which directly depends on the interface scattering intensity, that is, the interface reflection probability. If the particles reflect at the interface, we will set its $v_\parallel^{\text{new}}$ as $-v_\parallel$. In Fig. 1(e), as the interface reflection probability increases, the interface temperature jump increases rapidly. Moreover, it can be seen from the subgraph that the ratio of the interface temperature jump to the temperature difference of two thermal sources is independent of the external temperature difference. The introduction of the interface reflection probability enables us to simulate the quasi-one-dimensional thermal conduction under the different interface conditions.

We introduce a positive temperature-dependent ITR in the homogeneous system. The positive temperature-dependent ITR increases with the increasing interface temperature, which is different from the usual ITR. Such ITR is common in a homogeneous junction system composed of a negative thermal expansion material.[17] The volume of the material with the negative thermal expansion property decreases with increasing temperature, so the pressure at the interface will also decreases, and eventually the interface will gradually separate. The functional form of this kind of ITR (changes with temperature) usually has the approximate sigmoid function form. In this Letter, we use the hyperbolic tangent function to describe the relation between the interface reflection

probability and the interface average temperature:

$$P = 0.5[\tanh(\overline{T}_{\rm i} - 3.5) + 1], \tag{6}$$

where $\overline{T}_{\rm i}$ represents the average value of the temperature at the interface of two surfaces, and the function image is drawn in the inset of Fig. 2. The temperature of the left and right thermal sources is set as: $T_{\rm L} = T + dT$, $T_{\rm R} = T - dT$, $dT = 0.1$. The positive temperature-dependent interface thermal resistance exhibited by the interface reflection probability has the same temperature-dependent characteristics as the interface thermal resistance introduced in Ref. [17]. The reduction in effective thermal conductivity (ETC) at high temperature is obvious. Moreover, adjusting the peak temperature of ETC and the reduction range of ETC is very easy, only by adjusting the length ratio of the two segments or the initial external pressure. The length ratio of the two segments is used to adjust the average interface temperature, and the initial external pressure is used to reduce the ITR coming from interface separation.

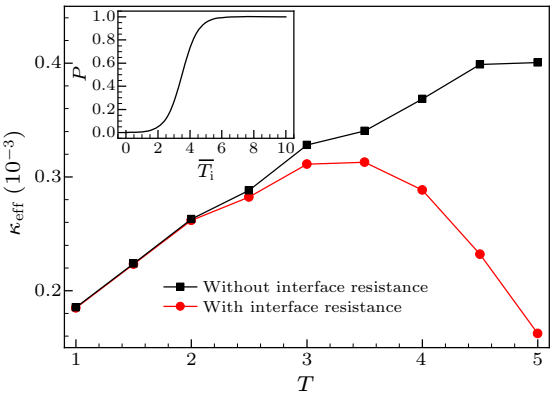

Fig. 2. The effective thermal conductivity of homojunction is a function of the model temperature. The temperature setting of thermal source is as follows: $T_{\rm L} = T + dT$, $T_{\rm R} = T - dT$, $dT = 0.1$. In the figure, red (black) represents the case with (without) the interface thermal resistance. The relationship between the interface reflection probability and the average interface temperature is shown in the inset.

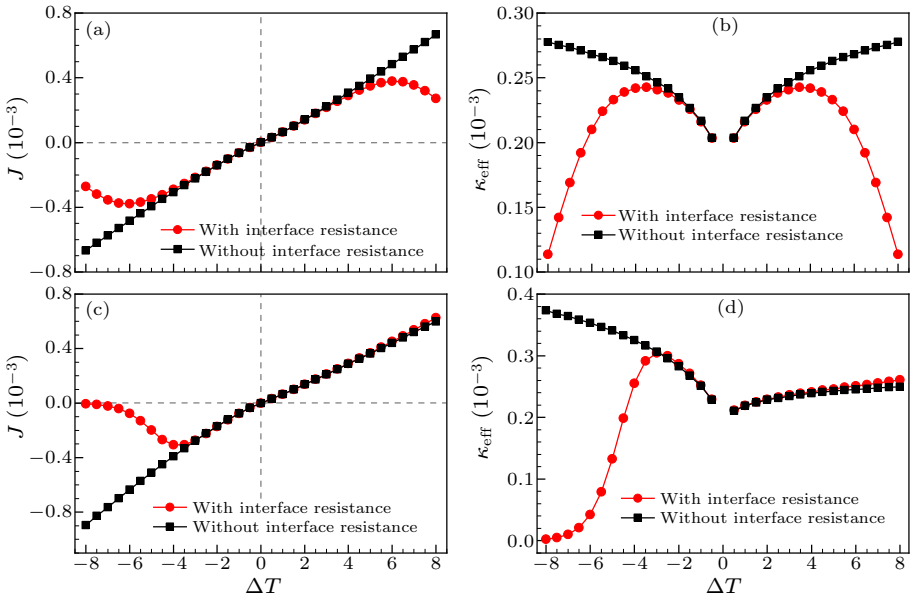

Fig. 3. (a) and (c) Thermal flow is a function of the external temperature difference for homojunction and heterojunction. (b) and (d) The effective thermal conductivity is a function of the external temperature difference for homojunction and heterojunction. The red and black lines represent the cases with and without the interface thermal resistance, respectively. The thermal source temperature at both ends of the material is set to $T_{\rm L} = 1$ ($T_{\rm R} = 1$) and $T_{\rm R} = 1 + \Delta T$ ($T_{\rm L} = 1 + \Delta T$) when $\Delta T > 0$ ($\Delta T < 0$).

Besides having the unimodal thermal conductivity characteristic, such a system is usually accompanied by the NDTR effect.[11,13–15,17] The NDTR effect means that when the temperature difference between the two ends of the material increases, the thermal flow does not increase monotonously. Therefore, we set the thermal source temperature at both ends: $T_{\rm L}$=1 ($T_{\rm R} = 1$) and $T_{\rm R} = 1 + \Delta T$ ($T_{\rm L} = 1 + \Delta T$) when $\Delta T > 0$ ($\Delta T < 0$). The thermal flow and ETC of the homojunction are plotted in Figs. 3(a) and 3(b). A non-monotonically increasing thermal flow is clearly visible, which is consistent with the finite element calculation.[17] Simultaneously, the rapidly decreasing ETC also appears with the NDTR effect under a large temperature difference. If the thermal flow direction is fixed, the ETC will also be in a unimodal form.

In the above paragraph, we mention to change the length ratio of the two segments of the homojunction mainly by adjusting the temperature at the interface and regulating the peak of ETC. There are many ways to achieve this goal, such as constructing a heterojunc-

tion. We calculate the structure shown in Fig. 1(c), furthermore, the thermal flow and ETC of the heterojunction are plotted in Figs. 3(c) and 3(d). As a result, we use heterojunction to construct an anisotropic thermal transport system: when a temperature difference is applied in a certain direction, the thermal flow is not hindered. However, when the temperature difference is reversed, the thermal flow in the system has a maximum value. The maximum value can be adjusted by the asymmetry of the system, which is also the most direct way to construct a thermal protector.

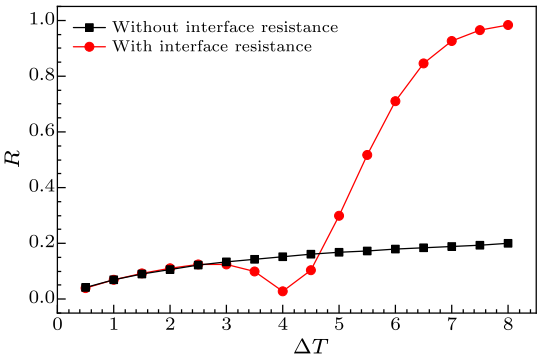

Fig. 4. Thermal rectification factor is a function of the external temperature difference for the heterojunction model. The red and black lines represent the cases with and without the interface thermal resistance, respectively.

For the heterojunction, the thermal flow has a strong anisotropy under a large temperature difference, which is very worthy of attention. Devices with strong anisotropic thermal flow are called thermal rectifiers. If the difference between the two directions is very large, a thermal diode can be realized.[1–5] We calculate the thermal rectification factor R in the heterojunction with the following formula:[4]

$$R = \left| \frac{J_+ - J_-}{J_+ + J_-} \right|, \tag{7}$$

where J_+ and J_- take the absolute value of the thermal flow with positive and negative temperature gradients. Therefore, for the symmetric thermal flow case of $J_+ = J_-$ ($R = 0$), there is no rectification effect. If only one of the thermal flow J_+/J_- vanishes, the rectification effect approaches to maximum with $R = 1$. According to the result in Fig. 4, the ITR can achieve strong thermal rectification under a large temperature difference, and the thermal flow in a certain direction is almost zero, which is approximately unidirectional. It is also well understood in physics that the heterojunction causes the interface temperature to deviate from the average temperature of the two thermal sources. The higher interface temperature causes the heterojunction to separate, so that thermal conduction no longer occurs. In particular, after considering the ITR, the thermal rectification ratio will no longer increase monotonically with the increase of the temperature difference, and even the thermal rectification effect almost disappears near certain temperature. This is because the unidirectional negative differential thermal resistance effect occurs in the direction of the original larger thermal flow, making this thermal flow gradually decrease to zero. Naturally, in this process, there will be a short-term phenomenon that the thermal flow in the two directions is almost equal, that is, the phenomenon of thermal rectification disappearing.

In summary, we have verified that the positive temperature-dependent interface thermal resistance is of great significance for achieving NDTR effect. The positive temperature-dependent interface thermal resistance can be realized by a homojunction/heterojunction made of materials with negative thermal expansion characteristics. In a homogeneous junction with a positive temperature-dependent interface thermal resistance, a pair of equivalent negative differential thermal resistance effects can be realized in different temperature gradient directions. Simultaneously, an easy-to-control unimodal thermal conductivity metamaterial is also naturally realized. Subsequently, in a heterojunction with a positive temperature-dependent interface thermal resistance, a pair of invaluable negative differential thermal resistance effects can be realized in different temperature gradient directions. Under certain conditions, the phenomenon of negative differential thermal resistance and normal interface thermal resistance can appear in different temperature gradient directions, respectively. In particular, the positive temperature-dependent interface thermal resistance in the heterojunction system also has strong anisotropy, which is very gratifying for us to manufacture high-performance thermal diodes. Our investigation is an important step in changing the understanding of interface thermal resistance and designing new thermal devices using interface thermal resistance.

References

[1] Terraneo M, Peyrard M and Casati G 2002 *Phys. Rev. Lett.* **88** 094302
[2] Li B, Wang L and Casati G 2004 *Phys. Rev. Lett.* **93** 184301
[3] Li B, Lan J and Wang L 2005 *Phys. Rev. Lett.* **95** 104302
[4] Yang Y, Chen H, Wang H, Li N and Zhang L 2018 *Phys. Rev. E* **98** 042131
[5] Wang H, Yang Y, Chen H, Li N and Zhang L 2019 *Phys. Rev. E* **99** 062111
[6] Jiang P, Hu S, Ouyang Y, Ren W, Yu C, Zhang Z and Chen J 2020 *J. Appl. Phys.* **127** 235101
[7] Zhang Z, Ouyang Y, Cheng Y, Chen J, Li N and Zhang G 2020 *Phys. Rep.* **860** 1
[8] Strohm C, Rikken G L J A and Wyder P 2005 *Phys. Rev. Lett.* **95** 155901
[9] Zhang L, Wang J and Li B 2009 *New J. Phys.* **11** 113038
[10] Zhang L 2016 *New J. Phys.* **18** 103039
[11] Li B, Wang L and Casati G 2006 *Appl. Phys. Lett.* **88**

143501
[12] He D, Buyukdagli S and Hu B 2009 *Phys. Rev. B* **80** 104302
[13] Hu J, Wang Y, Vallabhaneni A, Ruan X and Chen Y 2011 *Appl. Phys. Lett.* **99** 113101
[14] Joulain K, Drevillon J, Ezzahri Y and Ordonez-Miranda J 2016 *Phys. Rev. Lett.* **116** 200601
[15] Fornieri A, Timossi G, Bosisio R, Solinas P and Giazotto F 2016 *Phys. Rev. B* **93** 134508
[16] Criado-Sancho M and Jou D 2017 *J. Appl. Phys.* **121** 024503
[17] Yang Y, Ma D, Zhao Y and Zhang L 2020 *J. Appl. Phys.* **127** 195301
[18] Chang C, Okawa D, Majumdar A and Zettl A 2006 *Science* **314** 1121
[19] Wang H, Hu S, Takahashi K, Zhang X, Takamatsu H and Chen J 2017 *Nat. Commun.* **8** 1
[20] Pollack G 1969 *Rev. Mod. Phys.* **41** 48
[21] Swartz E and Pohl R 1989 *Rev. Mod. Phys.* **61** 605
[22] Swartz E and Pohl R 1987 *Appl. Phys. Lett.* **51** 2200
[23] Stoner R and Maris H 1993 *Phys. Rev. B* **48** 16373
[24] Costescu R, Wall M and Cahill D 2003 *Phys. Rev. B* **67** 054302
[25] Lyeo H and Cahill D 2006 *Phys. Rev. B* **73** 144301
[26] Chen Z, Jang W, Bao W, Lau C and Dames C 2009 *Appl. Phys. Lett.* **95** 161910
[27] Landry E and Mcgaughey A 2009 *Phys. Rev. B* **80** 165304
[28] Koh Y, Bae M, Cahill D and Pop E 2010 *Nano Lett.* **10** 4363
[29] Ye N, Feser J, Sadasivam S, Fisher T, Wang T, Ni C and Janotti A 2017 *Phys. Rev. B* **95** 085430
[30] Hohensee G, Wilson R and Cahill D 2015 *Nat. Commun.* **6** 6578
[31] Hsieh W, Lyons A, Pop E, Keblinski P and Cahill D 2011 *Phys. Rev. B* **84** 184107
[32] Alonso D, Artuso R, Casati G and Guarneri I 1999 *Phys. Rev. Lett.* **82** 1859
[33] Li B, Casati G and Wang J 2003 *Phys. Rev. E* **67** 021204
[34] Larralde H, Leyvraz F and Mejia-Monasterio C 2003 *J. Stat. Phys.* **113** 197
[35] Casati G, Mejia-Monasterio C and Prosen T 2007 *Phys. Rev. Lett.* **98** 104302
[36] Chen H, Wang H, Yang Y, Li N and Zhang L 2018 *Phys. Rev. E* **98** 032131
[37] Chen H, Yang Y, Yu Z, Zhong M and Zhang L 2020 *Phys. Rev. E* **101** 042129
[38] Hao Q, Chen G and Jeng M 2009 *J. Appl. Phys.* **106** 114321
[39] Hori T, Shiomi J and Dames C 2015 *Appl. Phys. Lett.* **106** 171901